

~~CONFIDENTIAL~~

2-9  
NACA RM L51L20

DL4831



TECH LIBRARY KAFB, NM

**NACA**

# RESEARCH MEMORANDUM

7306

PRESSURE MEASUREMENTS ON AN OGIVE-CYLINDER BODY

AT MACH NUMBER 4.04

By Douglas R. Lord and Edward F. Ulmann

Langley Aeronautical Laboratory  
Langley Field, Va.

Classification code: *Unclassified*

Re: *Priority of NASA Tech Pub Announcement #4*

By: *16 Mar 59*

By: *NK*

GRADE OF OFFICER MAKING CHANGE: *14 Mar 61* CLASSIFIED DOCUMENT

This material contains information affecting the National Defense of the United States within the meaning of the espionage laws, **DATEA**, U.S.C., Secs. 793 and 794, the transmission or revelation of which in any manner to unauthorized person is prohibited by law.

## NATIONAL ADVISORY COMMITTEE FOR AERONAUTICS

WASHINGTON

February 26, 1952

~~CONFIDENTIAL~~

*319.98/13*



## NATIONAL ADVISORY COMMITTEE FOR AERONAUTICS

## RESEARCH MEMORANDUM

## PRESSURE MEASUREMENTS ON AN OGIVE-CYLINDER BODY

AT MACH NUMBER 4.04

By Douglas R. Lord and Edward F. Ulmann

## SUMMARY

Pressure-distribution tests on an ogive-cylinder configuration with and without longitudinal spoilers were made at a Mach number of 4.04 and a Reynolds number, based on body length, of  $19 \times 10^6$ . The presence of the spoilers caused no noticeable change in the body pressures in regions which contribute the greatest amount of body normal force. The experimental pressures over the smooth body gave excellent agreement at an angle of attack of  $0^\circ$  with the characteristic theory predictions and agreed fairly well on the windward side of the body at angles of attack up to  $30^\circ$  with the hypersonic approximation including the effects of centrifugal force. A region of separated cross flow over the lee side of the body was indicated by the pressure measurements and by a surface-flow-visualization technique. The section cross-flow drag coefficients determined from the flow about the cylindrical afterbody were in good agreement with the drag coefficients of an unswept circular cylinder when the cross component of the Mach number was supersonic.

## INTRODUCTION

Preliminary force and moment tests on an ogive-cylinder configuration - a proposed body shape of the Hermes A-2 missile - at a Mach number of 4.04 were made to determine whether a reduction occurred in the rate of normal-force increase with increasing angle of attack similar to the reduction observed when the cross-flow Reynolds number reached the critical range in subsonic normal flow. In anticipation of this effect it was proposed to use spoilers on the body. These spoilers would cause a separation of the turbulent boundary layer which would increase the normal force over the body nose and would permit the use of smaller control surfaces for a given angle-of-attack change. These tests showed no reduction in the normal-force-curve slope with increasing angle of attack and showed that the presence of longitudinal spoilers had only a small effect on the normal force and the center-of-pressure position on the body. As an

extension of those tests, an investigation was conducted in the Langley 9- by 9-inch Mach number 4 blowdown tunnel to determine the pressure distributions on the smooth body as compared to those predicted by the available theories. Another purpose of the investigation was to determine whether spoilers, having a maximum spanwise projection of 0.044 body diameters, would cause any compensating effects on the pressures over the body surface which would not appear in the force measurements. Total pressures were measured in the vicinity of the body and liquid film tests were made on the body surface to investigate separation effects in the lee of the body. The models were tested at angles of attack up to 30° at a Mach number of 4.04, and at a Reynolds number, based on body length, of  $19 \times 10^6$ .

## SYMBOLS

p	stream static pressure
$p_t$	total pressure
M	stream Mach number
$M_c$	component of stream Mach number normal to model axis
$\gamma$	ratio of specific heats of air (1.4)
q	stream dynamic pressure $\left(\frac{\gamma}{2} \rho M^2\right)$
$p_l$	local static pressure on surface of model
P	pressure coefficient $\left(\frac{p_l - p}{q}\right)$
$\Delta P$	increment of pressure coefficient due to angle of attack
x, r, $\theta$	cylindrical coordinates ( $\theta = 0^\circ$ in plane of angle of attack and on the windward side)
$\alpha$	angle of attack
$\Lambda$	minimum angle between stream direction and a plane tangent to body surface at a specified point

R	Reynolds number, based on body length
$R_c$	cross-flow Reynolds number, based on the normal component of the velocity and the body diameter
$l$	body length
$c_{d_c}$	section drag coefficient of a circular cylinder

#### APPARATUS AND TESTS

The tests were conducted in the Langley 9- by 9-inch Mach number 4 blowdown tunnel. For these tests a pressure-regulating valve held the settling-chamber pressure at 250 pounds per square inch absolute. This pressure and the corresponding air temperature were continuously recorded on film during each run. The absolute humidity of the air used was always below  $9.0 \times 10^{-6}$  pounds of water vapor per pound of dry air.

The basic ogive-cylinder model was 9 inches long and had a maximum diameter of 1 inch (fig. 1). Two pressure-distribution models were constructed by the General Electric Company, one a smooth body of revolution and the other having spoilers with a maximum spanwise projection of 0.044 inch (see fig. 2). Each model had 35 pressure orifices of 0.052-inch diameter located in one longitudinal and five circumferential rows, as tabulated in figure 1. The orifices were connected to a mercury-manometer board and the pressures were recorded photographically. Another model without spoilers or orifices was constructed by the Langley laboratory for flow-visualization tests and was later modified by the installation of a total-pressure tube mounted from the surface to determine whether axial separation had occurred in the lee of the body. The nose of this tube was located at the 72.2-percent-body-length station and was 0.19 body diameters from the model surface as shown by the dotted outline in figure 1.

All three models were mounted on 5/8-inch-diameter stings so that the bases of the models were 3 inches ahead of the support struts (see fig. 3). Angle-of-attack changes were made by rotating the model in pitch about the one-half-body-length position.

The pressure-distribution models were tested at angles of attack of approximately  $0^\circ$ ,  $5^\circ$ ,  $10^\circ$ ,  $15^\circ$ ,  $20^\circ$ , and  $30^\circ$ . The pressure-distribution model without spoilers was tested with the longitudinal row of orifices mounted at  $\theta = 0^\circ$ ,  $45^\circ$ ,  $90^\circ$ ,  $180^\circ$ ,  $225^\circ$ , and  $270^\circ$ ; whereas the model with spoilers was tested with the longitudinal row

located only at  $\theta = 0^\circ$  and  $180^\circ$ . Flow-visualization tests were made on the smooth model by using the china-clay surface-flow-visualization technique of reference 1 at angles of attack of  $0^\circ$ ,  $5^\circ$ ,  $10^\circ$ ,  $20^\circ$ , and  $30^\circ$ . Total-pressure surveys were made around the smooth model at angles of attack of  $15^\circ$ ,  $20^\circ$ , and  $30^\circ$ . A schlieren photograph was taken during each run and the true angles of attack were determined from the schlieren negatives by use of an optical comparator. The changes in angle of attack due to the aerodynamic loads were found to be negligible. The Reynolds number based on body length was  $19 \times 10^6$  for all tests.

#### PRECISION OF DATA

The flow conditions in the tunnel test section are described in reference 2. The weak shocks which were found to exist in the test section have a localized effect on the model pressures which will be pointed out later. The accuracy of the pressure coefficients presented, when the local effects of the tunnel pressure irregularities are neglected, is about  $\pm 0.01$ . This value was determined by taking into account the repeatability of points and the limitations of the measuring and computing methods used.

#### RESULTS AND DISCUSSION

Effect of spoilers.- Figure 4 presents the circumferential pressure distributions at 35.5-percent-body length from the missile nose for both models. No effect of the spoilers, which project 0.028 body diameters at this station, could be identified here or at any other station, the variation in pressure coefficient at any point being within the accuracy of the measurements. The change in pressure coefficient near the spoiler location which might be expected in conjunction with the very slight increase in normal force found in the preliminary tests was not observed due to the lack of orifices in this region. This lack of orifices in the immediate vicinity of the spoilers is not considered significant, since changes in pressure at the sides of the body have little effect on the body normal force due to the small projected area over which they act. If the action of the spoilers had caused any large change in the normal force of the body, the pressures measured by the existing orifices in the lee of the body would have changed considerably. The normal-force and pitching-moment coefficients determined from the integrated pressure distributions over the bare body were in excellent agreement with the coefficients determined from the preliminary force tests.

Comparison of experiment with theory.- Comparisons of the experimental longitudinal pressure distributions at  $\alpha = 0^\circ$  over the smooth model with those computed by the small-disturbance method of reference 3, by the method of characteristics, and by the hypersonic approximation without centrifugal force (reference 4) are presented in figure 5. The characteristic theory accurately predicts the pressures over the body and the hypersonic approximation  $P = 2 \sin^2 \Lambda$  gives a surprisingly good prediction, although failing, of course, to predict any negative pressure coefficients. If any of the effects of centrifugal force as presented in reference 4 were included, the hypersonic approximation would give poorer agreement with experiment over the ogival nose.

The small-disturbance theory can give no results near the nose of this body at Mach number 4, since the angle between the surface tangent at the apex and the body axis is greater than the Mach angle. This theory gives a relatively poor prediction of the body pressure coefficients in the region of the juncture of the ogive and the cylinder. At angles of attack the small-disturbance theory of reference 3 is not applicable and the computations required for the characteristic theory become very laborious. For these reasons these theories were used only at  $\alpha = 0^\circ$ .

A method for predicting the increment of pressure coefficient due to angle of attack has been developed in reference 5 and independently in reference 6. In the latter method, the linearized theory was used to estimate the velocity field around the body. Velocity components associated with thickness and angle of attack were independently calculated and superimposed on the free-stream-velocity components. The pressure distribution was then evaluated from the resultant velocity field. The results of this improved linearized theory in predicting the incremental pressure coefficients at  $\alpha = 5^\circ$  for several circumferential positions on the smooth body are compared in figure 6 with those obtained experimentally. The theoretical method gives a fair prediction of the experimental incremental pressure coefficients. Comparisons between the experimental and theoretical incremental pressure coefficients at higher angles of attack gave poorer agreement, as would be expected, since the assumption of incompressible cross Mach number in the development of the method is violated at the higher angles of attack for this test Mach number.

In contrast to the previously mentioned method and the small-disturbance theory, the hypersonic approximation of reference 4 can be used throughout the angle-of-attack range of these tests. It should be realized that its predictions are more accurate at higher supersonic Mach numbers than that of these tests and that it cannot predict the pressures in the lee of the body. Nevertheless, it is used to predict the pressures over the test body, since it is the most practical method

available for predicting pressures on ogive-cylinder bodies at all angles of attack. Figures 7 and 8 present comparisons of experimental longitudinal and semicircumferential pressure distributions with those computed by this method. Since the pressures over the afterbody (see fig. 7) are relatively constant, the semicircumferential comparison is presented only at  $x/l = 0.577$ . The experimental points at  $x/l = 0.077$  at  $\theta = 0^\circ$  (fig. 7) are obtained from the pressure distributions on the model with spoilers, since the orifice at this position on the smooth model was inoperative. The effect of the spoilers on the pressures at this orifice is assumed to be negligible, since the spoilers have a span of only a few thousandths of an inch at this station and are located at  $90^\circ$  from the orifice. A slight increase in pressure near the  $x/l = 0.7$  station for  $\theta = 0^\circ$  and  $45^\circ$  can be seen in figure 7 at the higher angles of attack as a result of the weak disturbances in the tunnel which were mentioned in the section entitled "Precision of Data." In figure 7 the predictions of the hypersonic approximation without centrifugal force are in fairly good agreement with experiment, except at the  $\theta = 90^\circ$  meridian over the afterbody. The inclusion of the effects of centrifugal force has no effect on the theoretical pressures at  $\theta = 0^\circ$  and  $90^\circ$ , but improves the predictions of the hypersonic approximations at other values of  $\theta$  (see fig. 8), especially at the higher angles of attack.

Flow separation and cross-flow effects. - The experimental circumferential pressure distributions at five longitudinal stations are presented in figure 9 for the six test angles of attack. The pressures increased on the windward side of the body with angle of attack. The circumferential pressure distributions over the lee side of the cylindrical afterbody at  $5^\circ$  and  $10^\circ$  angle of attack (figs. 9(b) and 9(c)) generally reached maximum negative values at  $\theta$ 's of about  $135^\circ$  and  $225^\circ$  and become more positive at the  $180^\circ$  meridian. This pressure contour is similar to those obtained in references 6 to 8 on slender bodies at lower supersonic Mach numbers and is probably due to the action of the two symmetrically disposed vortices associated with cross-flow separation at low angles of attack.

At an angle of attack of  $15^\circ$  the circumferential pressure distributions at  $x/l = 0.688$  became flat in the lee of the body (fig. 9(d)). This flattening moved forward along the body as the angle of attack was increased until at  $\alpha = 30^\circ$  (fig. 9(f)) all the pressure distributions presented are flat in the lee of the body (additional points obtained farther forward but not presented showed that the pressure distribution in the lee of the body at  $\alpha = 30^\circ$  became flat as far forward as  $x/l = 0.133$ ). This flattening out of the circumferential pressure distributions on the lee side of the body is probably a result of the vortices drawing away from the body; thus the effect of the vortices on the body-surface pressures is lessened. This phenomenon has been previously discussed in reference 9 and is attributed to the similarity

between the development of the cross flow along the body with that of the flow about a circular cylinder impulsively started from rest.

Semicircumferential total-pressure surveys around the body at  $x/l = 0.722$  at 0.19 body diameters from the body surface for angles of attack of  $15^\circ$ ,  $20^\circ$ , and  $30^\circ$  are presented in figure 10. Check points which established the symmetry of the flow about the angle-of-attack plane were taken. The surveys at  $\alpha = 15^\circ$  and  $20^\circ$  indicated that in a region near  $\theta = 160^\circ$  the ratio of total pressure to free-stream pressure was lowest and that the ratio became somewhat greater at  $\theta = 180^\circ$ . At  $\alpha = 30^\circ$  the total pressures from  $150^\circ$  to  $180^\circ$  were relatively constant but at all angles they were more positive than stream-static pressure or model-surface pressure. This fact indicates that the total-pressure tube was not in a region of completely separated axial flow. These results are very similar to those obtained by the more complete total-pressure surveys of reference 6 at lower Mach numbers.

In order to further study the flow separation over the lee side of the body, tests were made using the china-clay lacquer technique described in reference 1. This technique indicates in shades of gray the relative rates of evaporation of the oil from a model surface. In general, white regions on a model indicate high evaporative rates and darker regions lower rates. The tests at  $\alpha = 0^\circ$  and  $\alpha = 5^\circ$  did not show any evidence of flow separation and are not presented. The photographs of the model following runs at angles of attack of  $10^\circ$ ,  $20^\circ$ , and  $30^\circ$  are presented in figure 11. The photographs show the surface of the model between the  $\theta = 0^\circ$  and  $\theta = 180^\circ$  positions. The model-surface appearance, however, was generally symmetrical with respect to the angle-of-attack plane. On the  $\alpha = 10^\circ$  photograph (fig. 11(a)) the nose region appeared to have a surplus coating of oil, as evidenced by the streaked appearance. On the  $\alpha = 20^\circ$  and  $\alpha = 30^\circ$  photographs (figs. 11(b) and 11(c)) the high shear stresses on the under side of the nose caused the china-clay lacquer coating to be blown off.

In the  $\alpha = 10^\circ$  photograph a longitudinal dark line is seen starting near the  $\theta = 180^\circ$  meridian forward and sloping down to the  $\theta = 90^\circ$  meridian aft which probably indicates the line of cross-flow separation similar to that reported in reference 6. This conclusion is reached since, at the point of cross-flow separation, the cross-flow velocity becomes zero at the body surface, while the axial component of the velocity does not separate. Thus along this line the rate of evaporation of the oil from the china-clay coating would be lessened and a dark line would appear. The area above this line indicates a somewhat slower rate of evaporation than below the line (see especially figure 11(b)), as would be expected. As the angle of attack was increased from  $10^\circ$  to  $20^\circ$ , the region of cross-flow separation apparently moved forward all the way to the nose of the model and the circumferential extent of the separated region on the afterbody decreased.

Further increasing the angle of attack to  $30^\circ$  caused little change in the cross-flow-separation region near the nose, although the separated region on the afterbody continued to diminish. The decrease in circumferential extent of the separated region on the afterbody is also indicated in the circumferential pressure distributions (fig. 9) by the decrease in extent of the flat parts of the curves for the  $x/l = 0.688$  station as the angle of attack approached  $30^\circ$ . In addition to the separation boundaries, the flow studies indicated four other longitudinal lines in the separated region, two on either side of the  $\theta = 180^\circ$  meridian of the body. Two of these lines are evident in figures 11(a) and 11(b) and are believed to be caused by the vortices in the separated region.

In order to check the similarity of the cross flow around the body to two-dimensional flow around a circular cylinder, the section normal-force coefficients for the 68.8-percent-body-length station were determined from the pressure distributions on the plain body and the cylindrical-section cross-flow drag coefficients were then determined for the cross components of Mach number at various angles of attack. A plot of the cylindrical-section cross-flow drag coefficients against the cross component of the stream Mach number for the 68.8-percent-body-length station is presented in figure 12. When this curve is compared with the curve of the drag coefficient of an unswept circular cylinder against Mach number taken from reference 10, the two curves show good agreement at Mach numbers greater than 1.0, despite the large differences in the Reynolds number of the tests and the differences in the test procedures. At Mach numbers less than 1.0, there is a large difference in the two curves, probably as a result of a combination of three effects. First, as pointed out in reference 6, at angles of attack of about  $5^\circ$  and  $10^\circ$  (corresponding to  $M_c = 0.35$  and  $M_c = 0.70$  in the present tests) the cross flow about a body of revolution is similar to the flow about a circular cylinder starting from rest and having traveled insufficient time for the development of steady-state flow. Reference 11 shows that the drag of a circular cylinder started from rest first increases to a value about twice the steady-state value and then decreases to the steady-state value. Thus it would be expected that the cross-flow drag coefficients at low cross-flow Mach numbers would be considerably higher than those obtained by Stanton (reference 10) and that the values of the cross-flow drag coefficients would decrease and approach the two-dimensional test values at higher Mach numbers, as is shown in figure 12. A second effect which probably prevents the pressure distributions about the body at low angles of attack from being truly representative of cylindrical cross flow even at the 68.8 percent body length station is the effect of the rather blunt nose. As a third possible reason for some of the disagreement, it should be pointed out that determining the section cross-flow drag coefficients from the section normal-force coefficients at the low angles of attack considerably amplifies the original inaccuracies in measurement.

CONFIDENTIAL  
CONCLUSIONS

Analysis of pressure-distribution tests of an ogive-cylinder with and without longitudinal spoilers, at Mach number 4.04 and a Reynolds number of  $19 \times 10^6$  indicated that:

1. The presence of the longitudinal spoilers caused no noticeable change in the pressures recorded over the regions of the body where the pressures contribute the greatest amount to the body normal force.

2. At an angle of attack of  $0^\circ$  the experimental pressures on the smooth body agreed very well with the prediction of the characteristic theory and fairly well with the predictions of the small-disturbance theory.

3. The improved linear-theory method of NACA TN 2044 gave good predictions of the incremental smooth-body pressures due to angle of attack as long as the cross-component of the Mach number was in the low subsonic range.

4. The hypersonic approximation with centrifugal force gave a good prediction of the pressure distribution over the windward parts of the smooth body throughout the angle-of-attack range of the tests.

5. Surface-flow-visualization tests verified the indication of the pressure measurements as to the existence and movement of a region of cross-flow separation over the lee side of the smooth body.

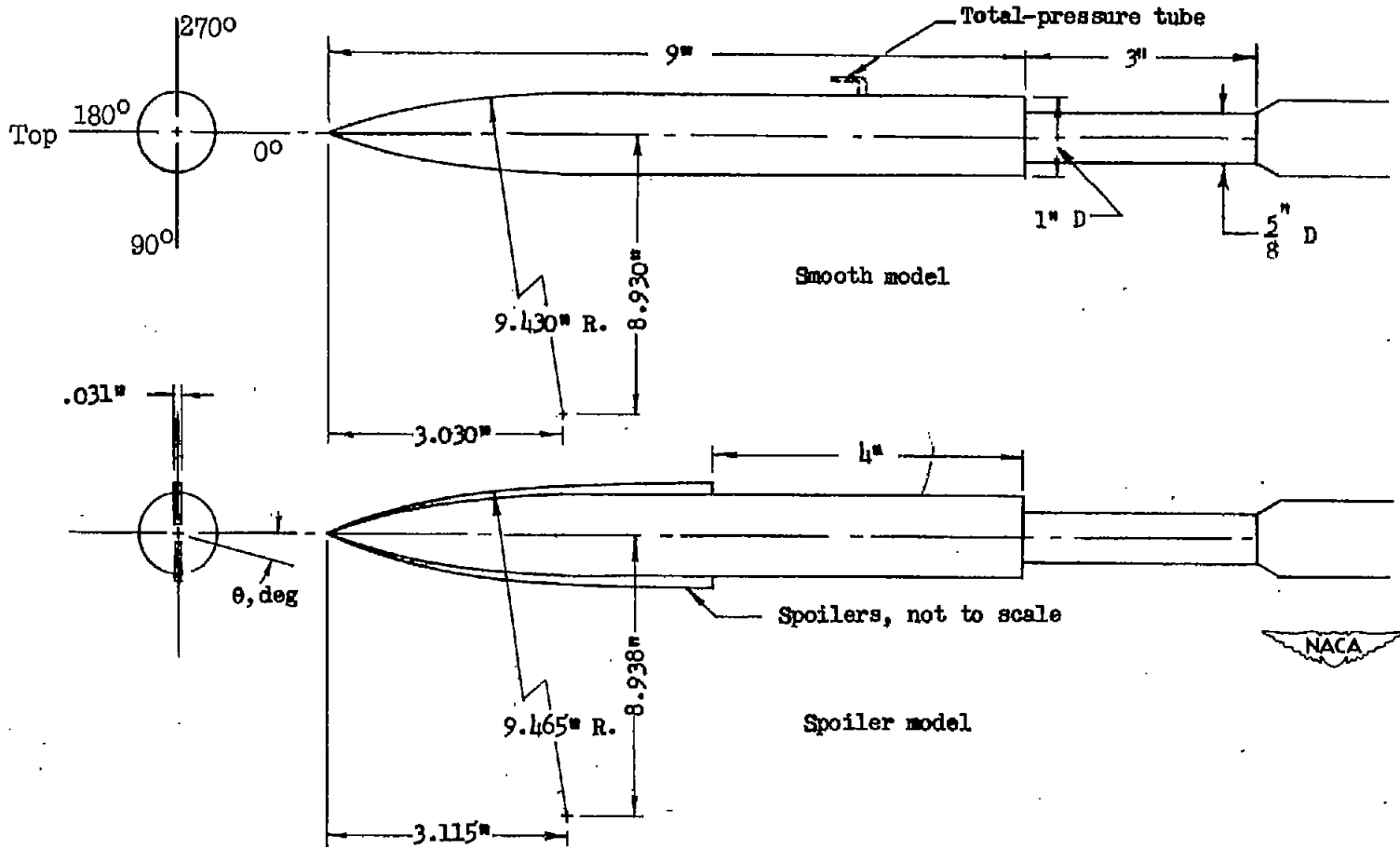
6. When the cross-component of the Mach number was supersonic the section cross-drag coefficients determined from the flow about the cylindrical afterbody at angles of attack agreed quite well with the drag coefficients previously found for unswept circular cylinders in supersonic flow.

Langley Aeronautical Laboratory  
National Advisory Committee for Aeronautics  
Langley Field, Va.

CONFIDENTIAL

## REFERENCES

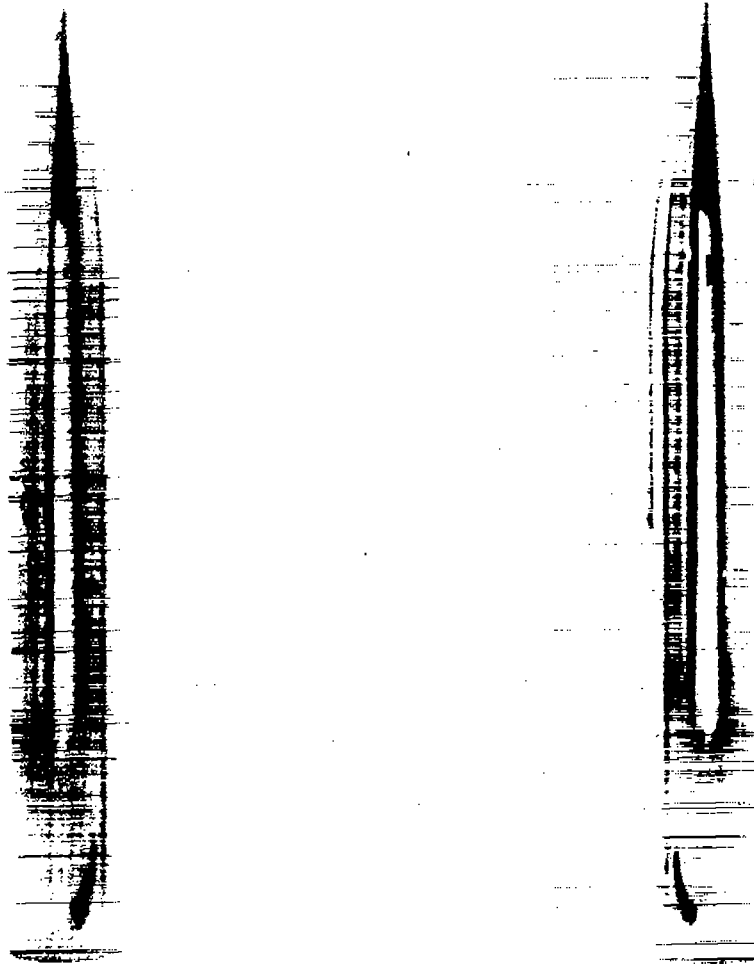
1. Gazley, C., Jr.: The Use of the China-Clay Lacquer Technique for Detecting Boundary-Layer Transition. Rep. No. R49A0536, Gen. Elec. Co., Mar. 1950.
2. Ulmann, Edward F., and Lord, Douglas R.: An Investigation of Flow Characteristics at Mach Number 4.04 over 6- and 9-Percent-Thick Symmetrical Circular-Arc Airfoils Having 30-Percent-Chord Trailing-Edge Flaps. NACA RM L51D30, 1951.
3. Von Kármán, Theodor, and Moore, Norton B.: Resistance of Slender Bodies Moving with Supersonic Velocities with Special Reference to Projectiles. Trans. A.S.M.E., vol. 54, no. 23, Dec. 15, 1932, pp. 303-310.
4. Griminger, G., Williams, E. P., and Young, G. B. W.: Lift on Inclined Bodies of Revolution in Hypersonic Flow. Jour. Aero. Sci., vol. 17, no. 11, Nov. 1950, pp. 675-690.
5. Allen, H. Julian: Pressure Distribution and Some Effects of Viscosity on Slender Inclined Bodies of Revolution. NACA TN 2044, 1950.
6. Luidens, Roger W., and Simon, Paul C.: Aerodynamic Characteristics of NACA RM-10 Missile in 8- by 6-Foot Supersonic Wind Tunnel at Mach Numbers from 1.49 to 1.98. I - Presentation and Analysis of Pressure Measurements (Stabilizing Fins Removed). NACA RM E50D10, 1950.
7. Jack, John R., and Burgess, Warren C.: Aerodynamics of Slender Bodies at Mach Number of 3.12 and Reynolds Numbers from  $2 \times 10^6$  to  $15 \times 10^6$ . I - Body of Revolution with Near-Parabolic Forebody and Cylindrical Afterbody. NACA RM E51H13, 1951.
8. Jack, John R.: Aerodynamic Characteristics of a Slender Cone-Cylinder Body of Revolution at a Mach Number of 3.85. NACA RM E51H17, 1951.
9. Allen, H. Julian, and Perkins, Edward W.: Characteristics of Flow over Inclined Bodies of Revolution. NACA RM A50L07, 1951.
10. Stanton, T. E.: On the Effect of Air Compression on Drag and Pressure Distribution in Cylinders of Infinite Aspect Ratio. R. & M. No. 1210, British A.R.C., 1929.
11. Schwabe, M.: Pressure Distribution in Nonuniform Two-Dimensional Flow. NACA TM 1039, 1943.



Orifice locations: (Longitudinal row at  $\theta = 0^\circ$ )

Station, $x/l$	0.077	0.133	0.188	0.244	0.311	0.355	0.410	0.466	0.521	0.577	0.633	0.688	0.744	0.799	0.854	0.912
$\theta$ , deg	0	0	0	0	0	0	0	0	0	0	0	0	0	0	0	0
					30	30		30		30		30				
					60	60		60		60		60				
					120	120		120		120		120				
						150						150				
						180						180				

Figure 1.-- Model dimensions and orifice locations.



Smooth model

Spoiler model

Figure 2.- Ogive-cylinder models with and without longitudinal spoilers.

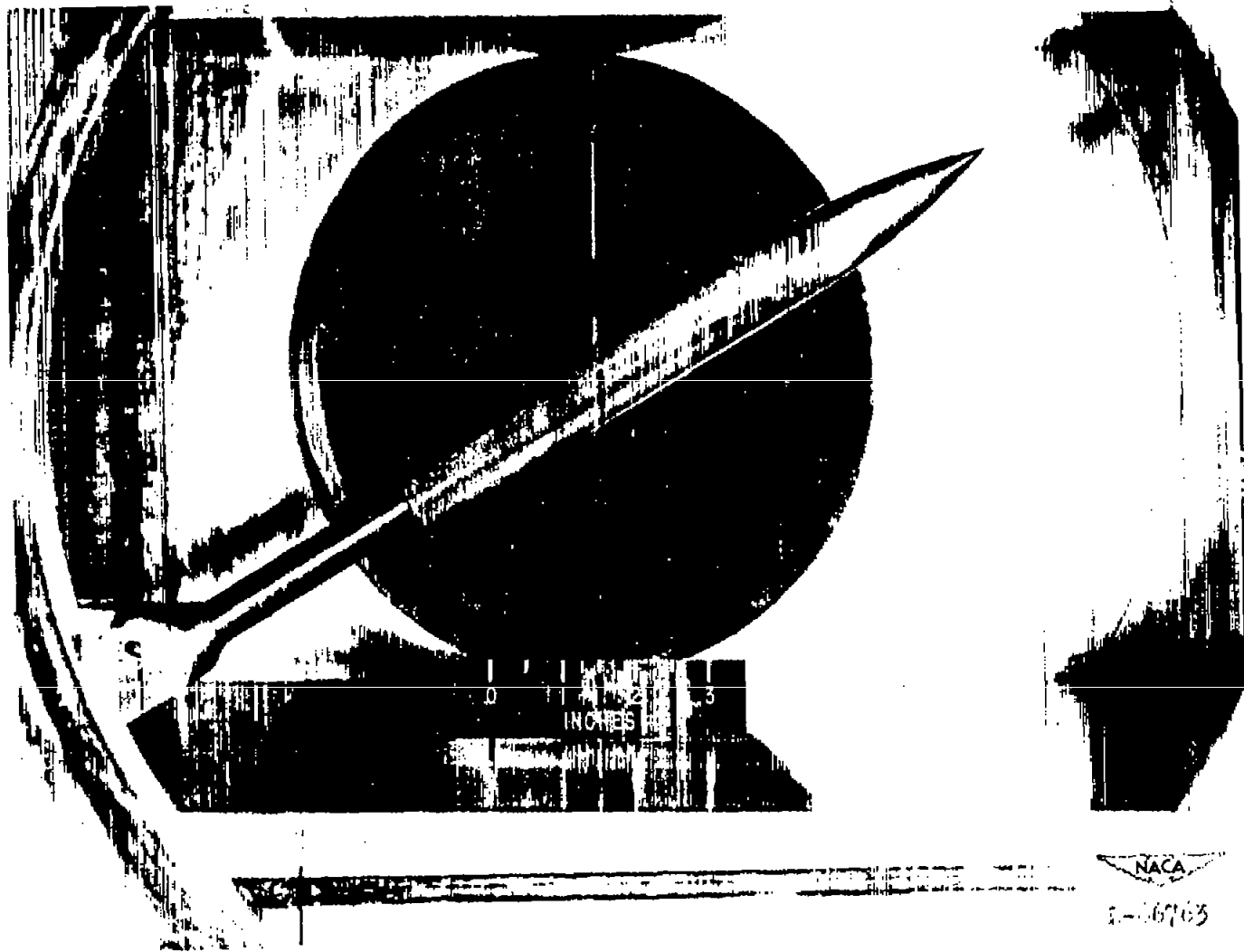


Figure 3.- Test section of Langley 9- by 9-inch Mach number 4 blowdown tunnel with ogive-cylinder model mounted on the sting.

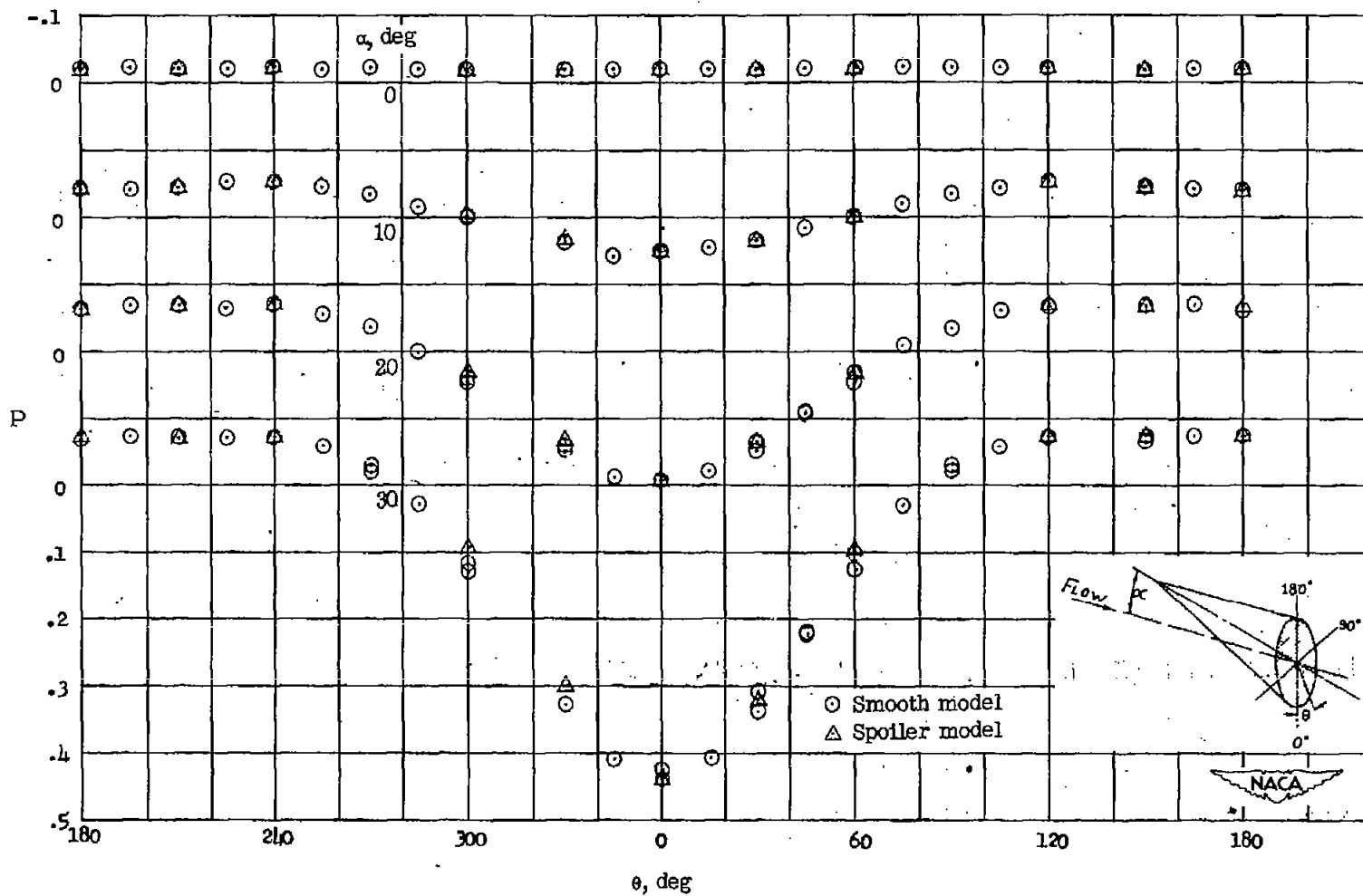


Figure 4.- Circumferential pressure distributions at the 35.5-percent-body-length station on the models with and without longitudinal spoilers.  $M = 4.04$ ;  $R = 19 \times 10^6$ .

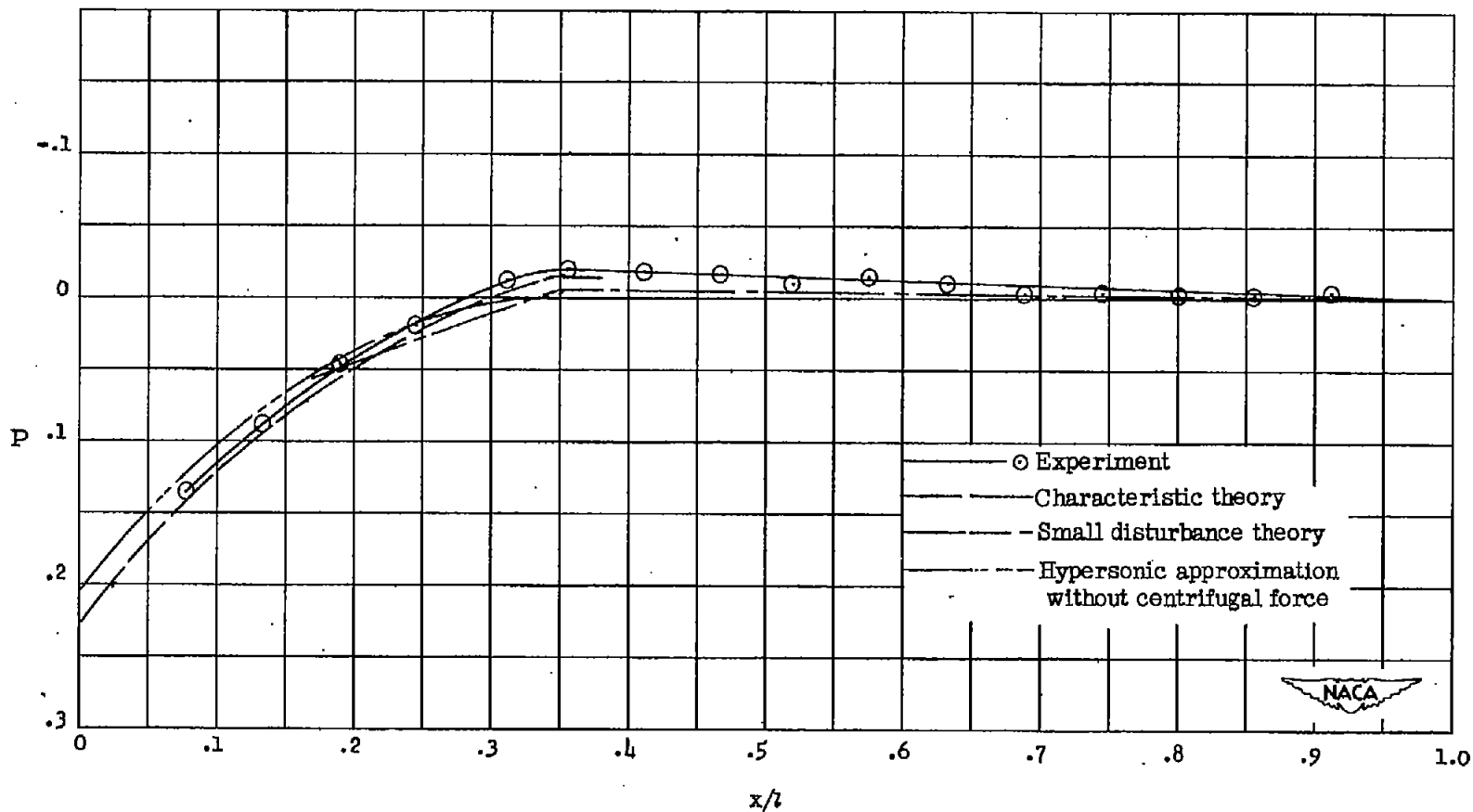


Figure 5.- Comparison of the experimental longitudinal pressure distribution at  $\alpha = 0^\circ$  with several theoretical methods.  $M = 4.04$ ;  
 $R = 19 \times 10^6$ .

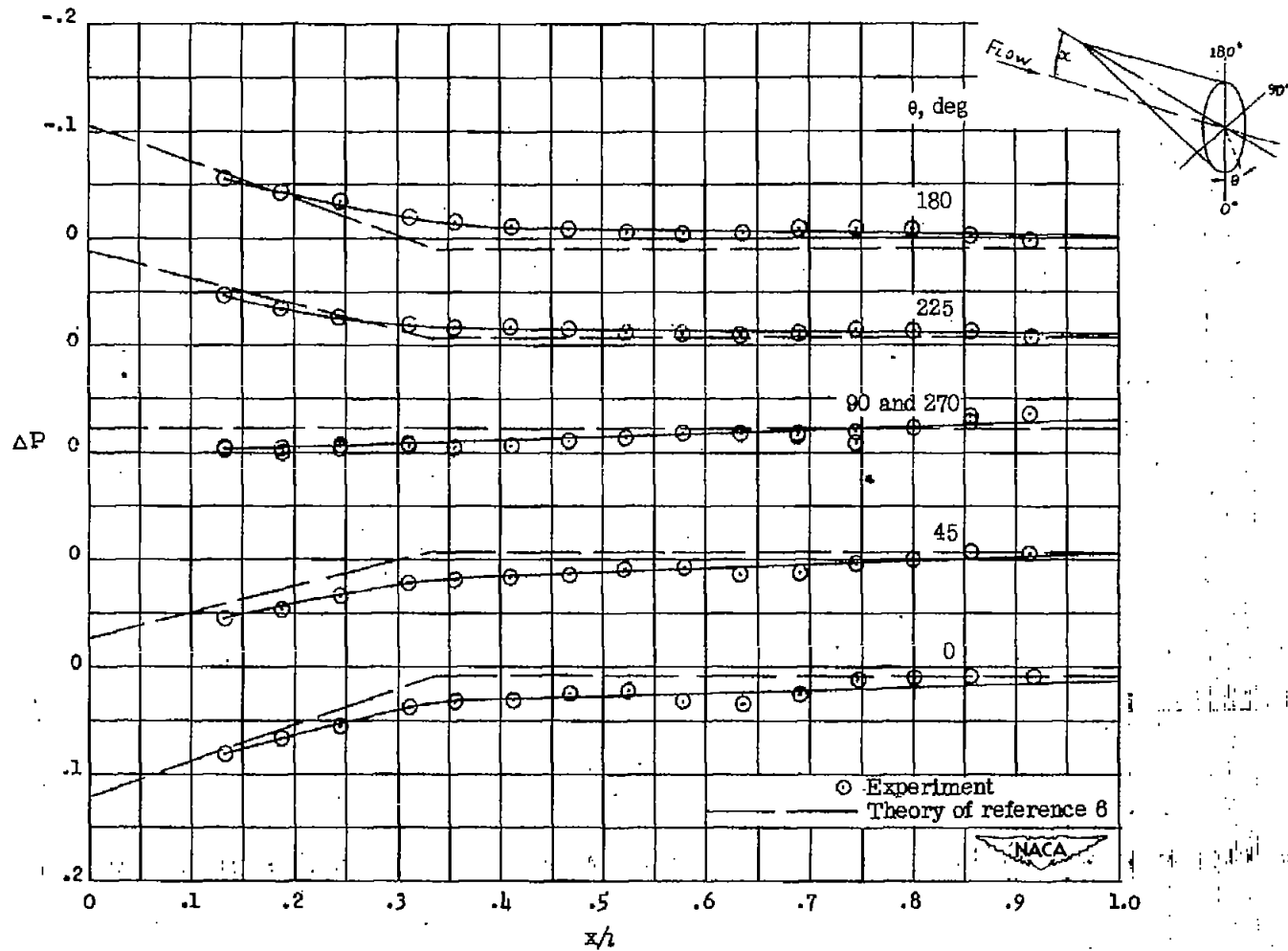
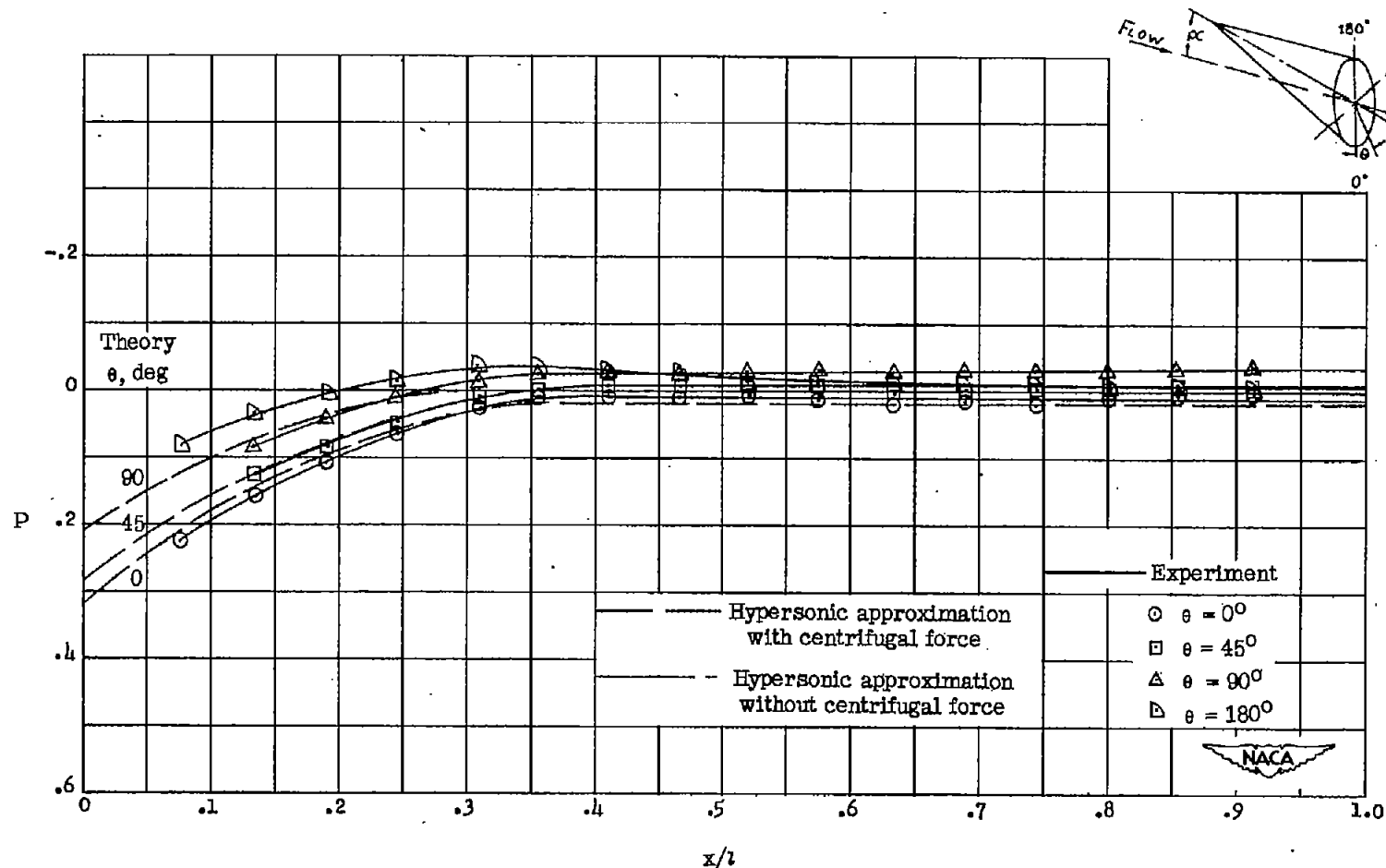
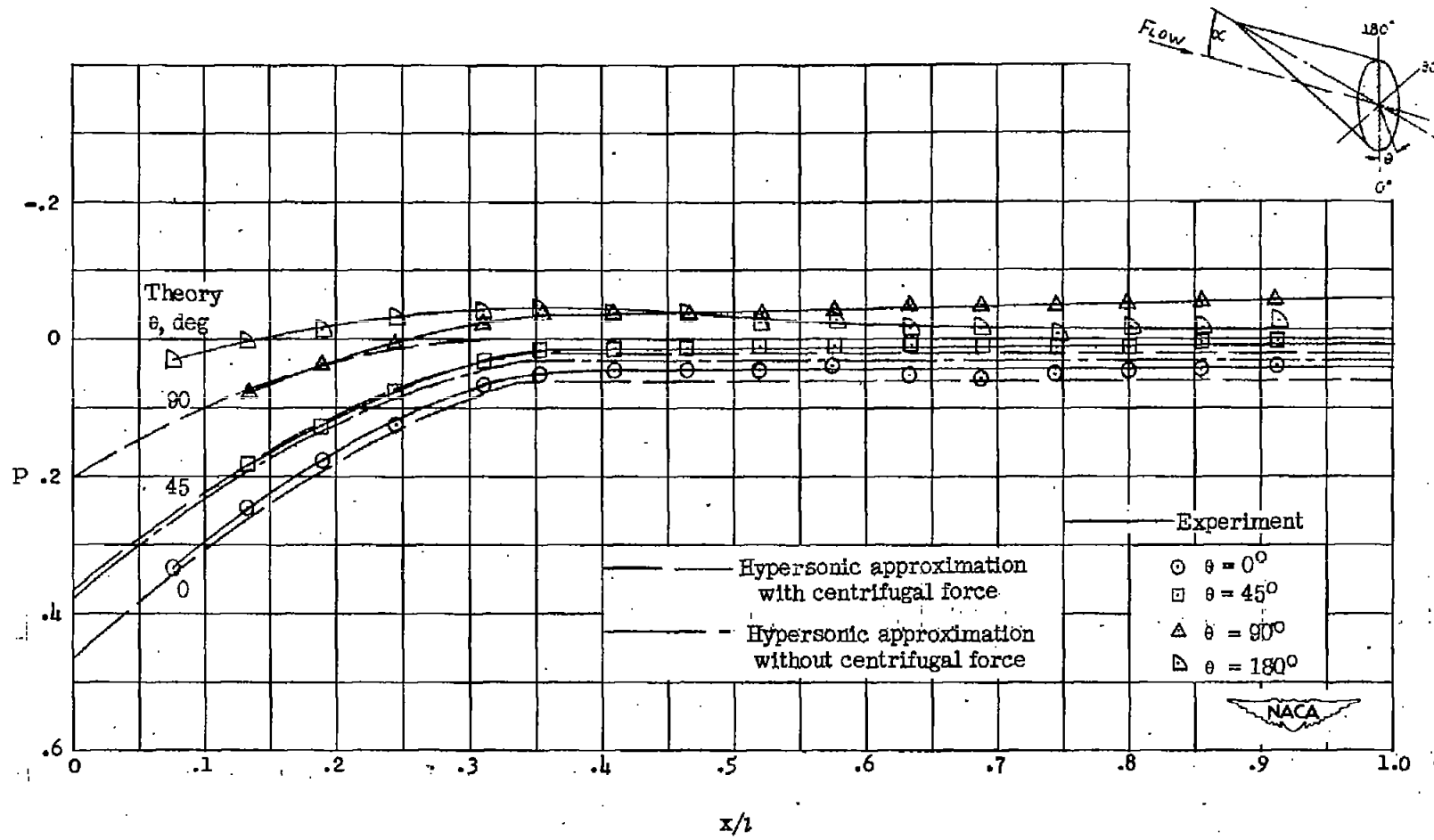


Figure 6.- Comparison between experimental and theoretical increment in pressure coefficient due to angle of attack for several circumferential positions.  $\alpha = 5^\circ$ ;  $M = 4.04$ ;  $R = 19 \times 10^6$ .



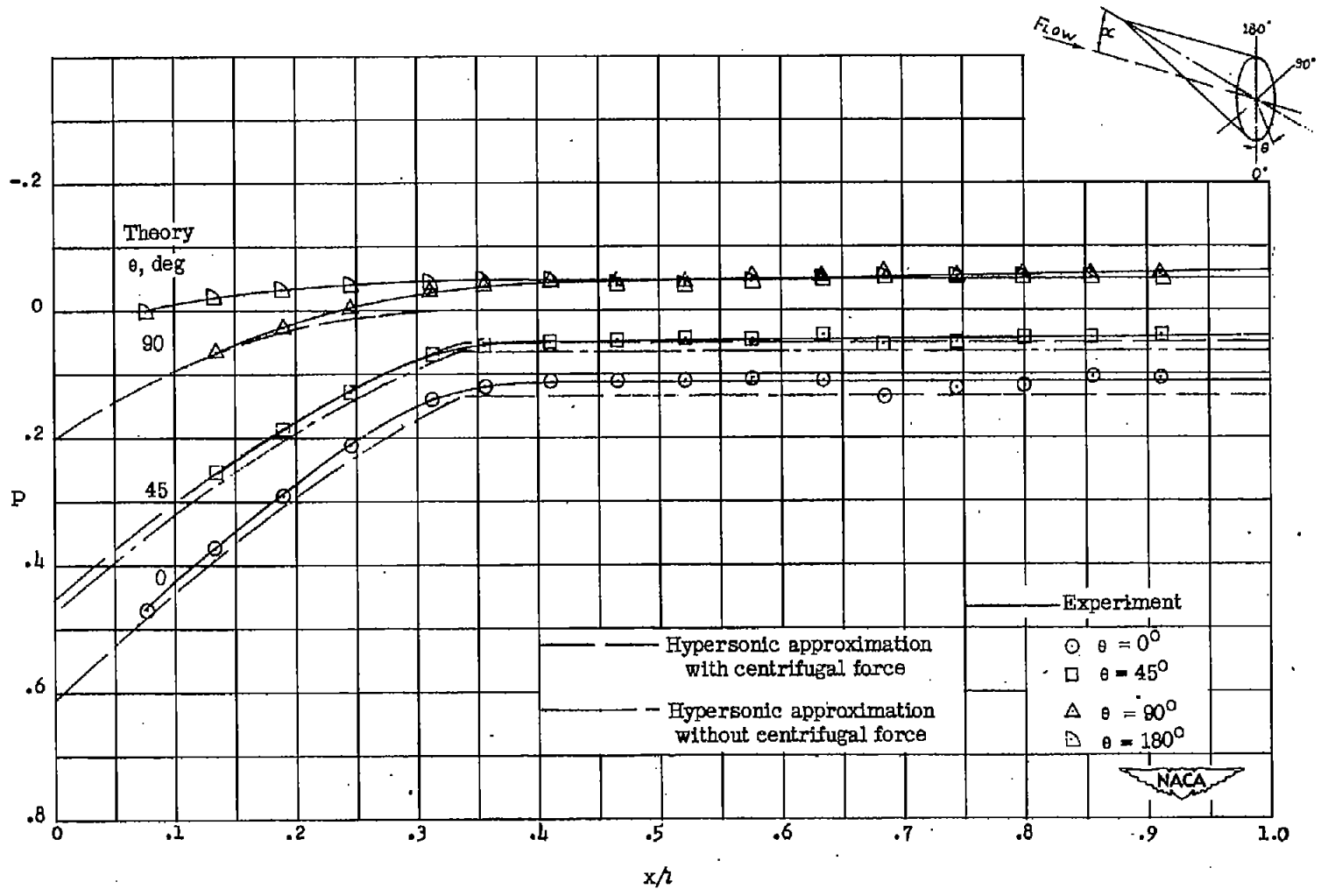
(a)  $\alpha = 5^\circ$ .

Figure 7.- Experimental and theoretical longitudinal pressure distributions for several circumferential positions.  $M = 4.04$ ;  
 $R = 19 \times 10^6$ .



(b)  $\alpha = 10^\circ$ .

Figure 7.- Continued.



(c)  $\alpha = 15^\circ$ .

Figure 7.- Continued.

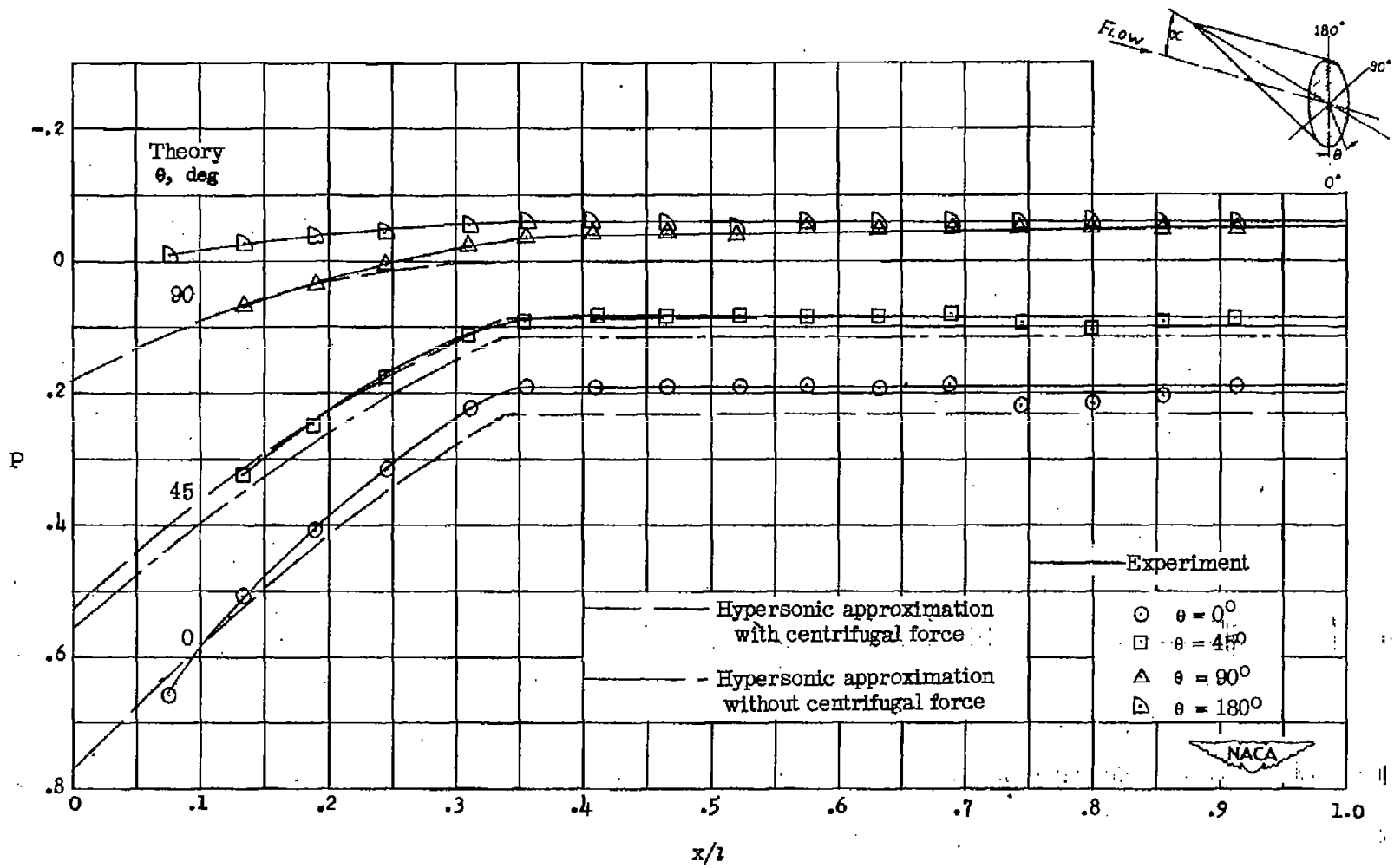
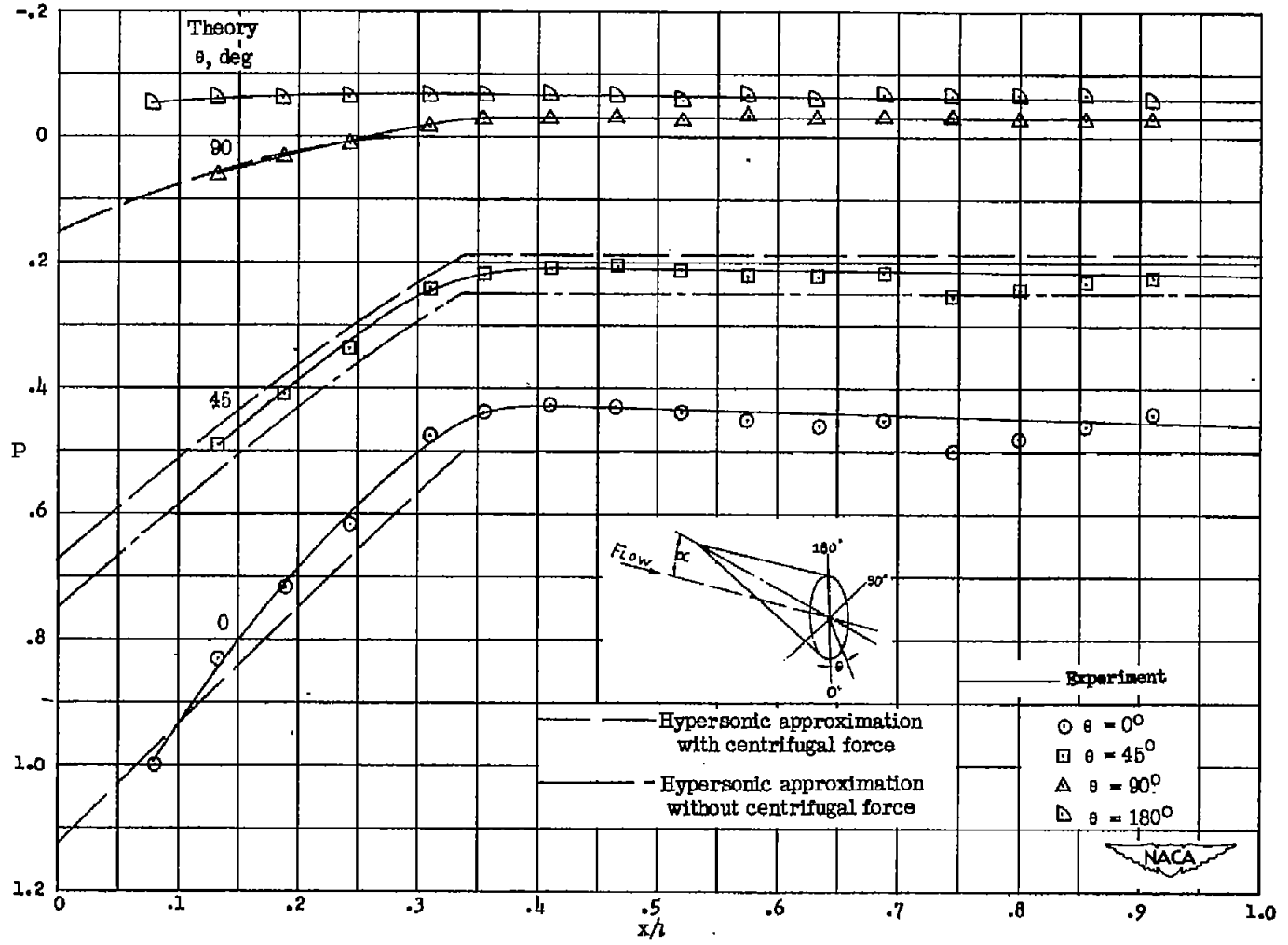
(d)  $\alpha = 20^\circ$ .

Figure 7.- Continued.



(e)  $\alpha = 30^\circ$ .

Figure 7.- Concluded.

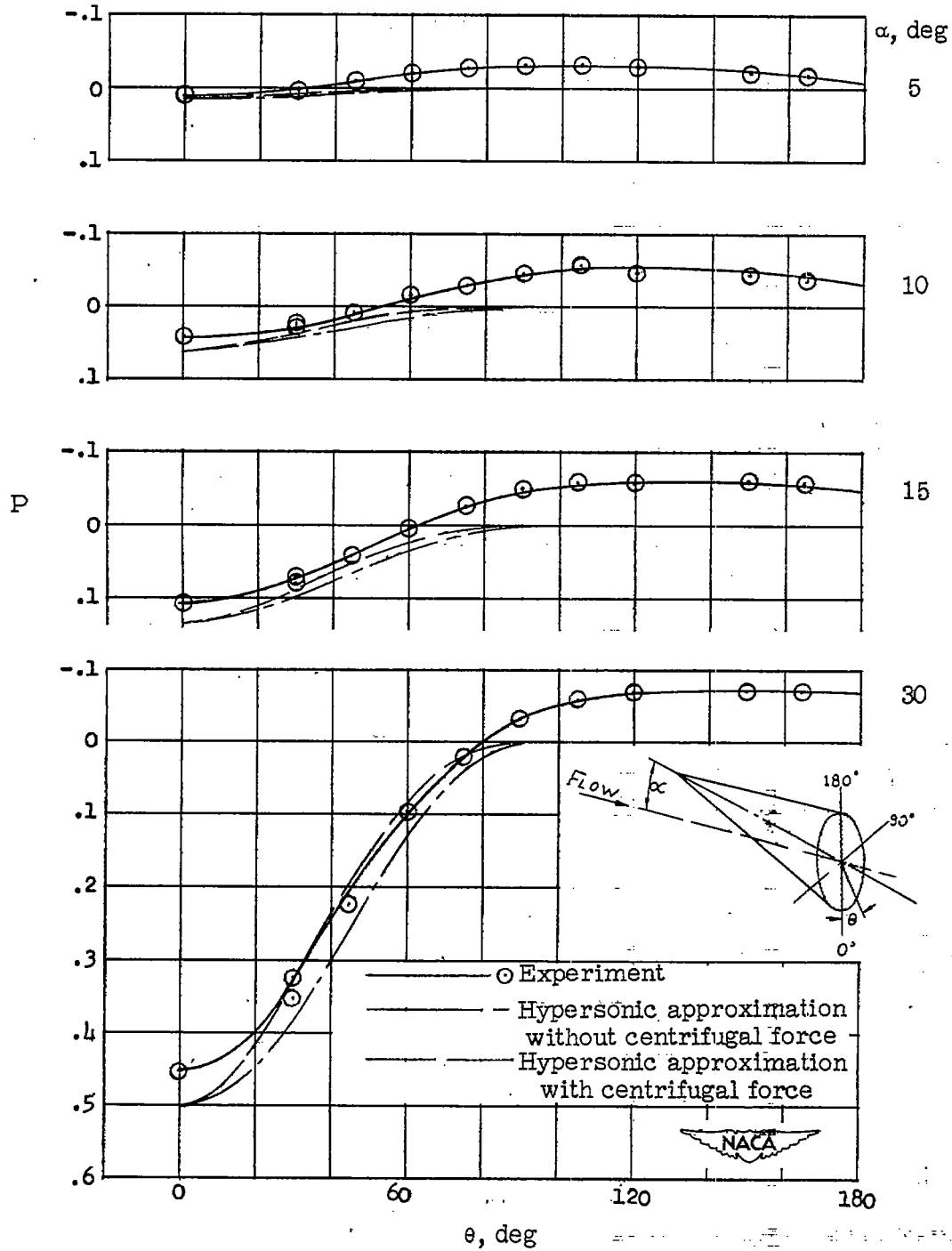


Figure 8.- Variation of the circumferential pressure distribution at the 57.7-percent body-length station with angle of attack.

$M = 4.04$ ;  $R = 19 \times 10^6$ .

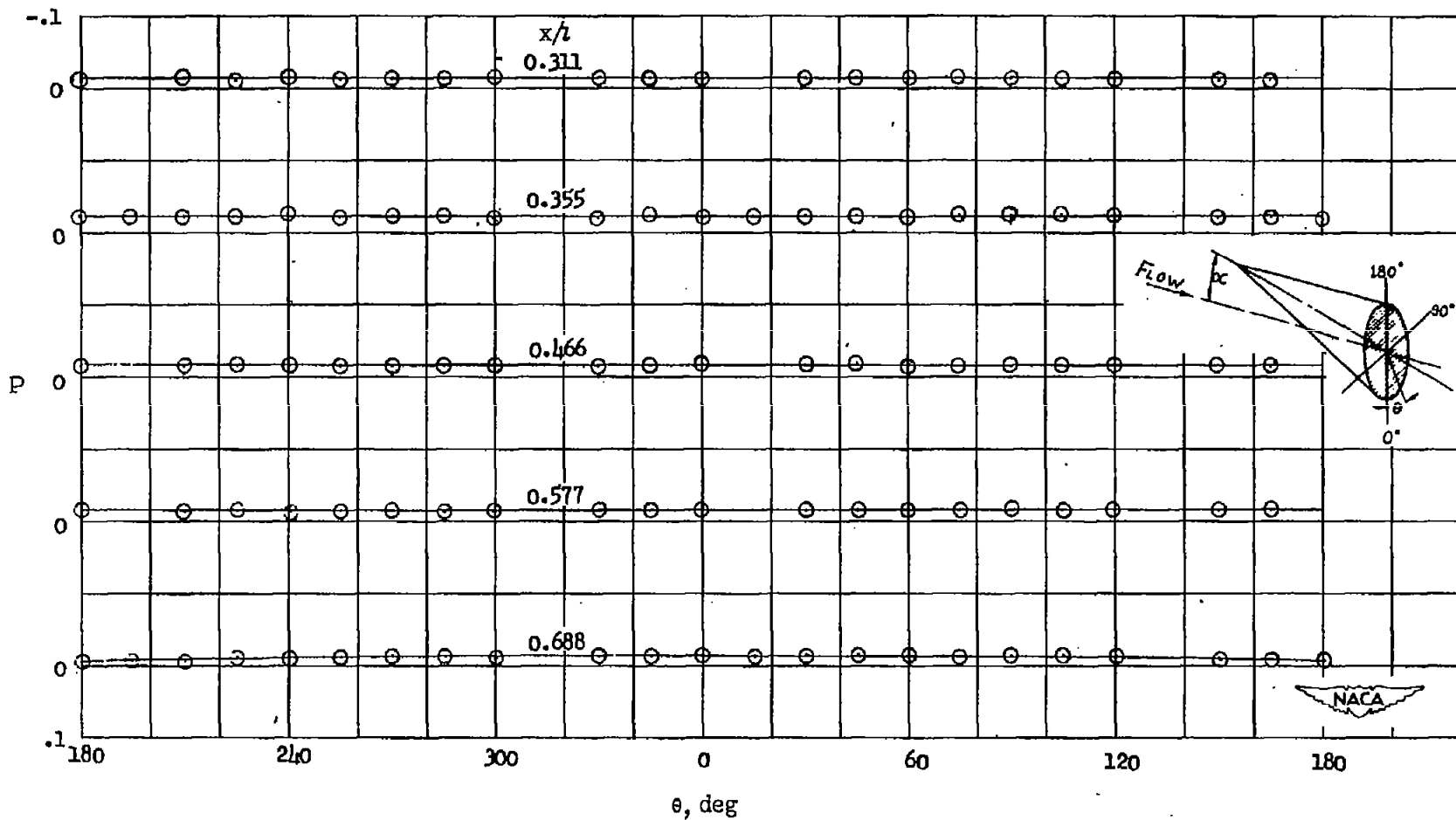
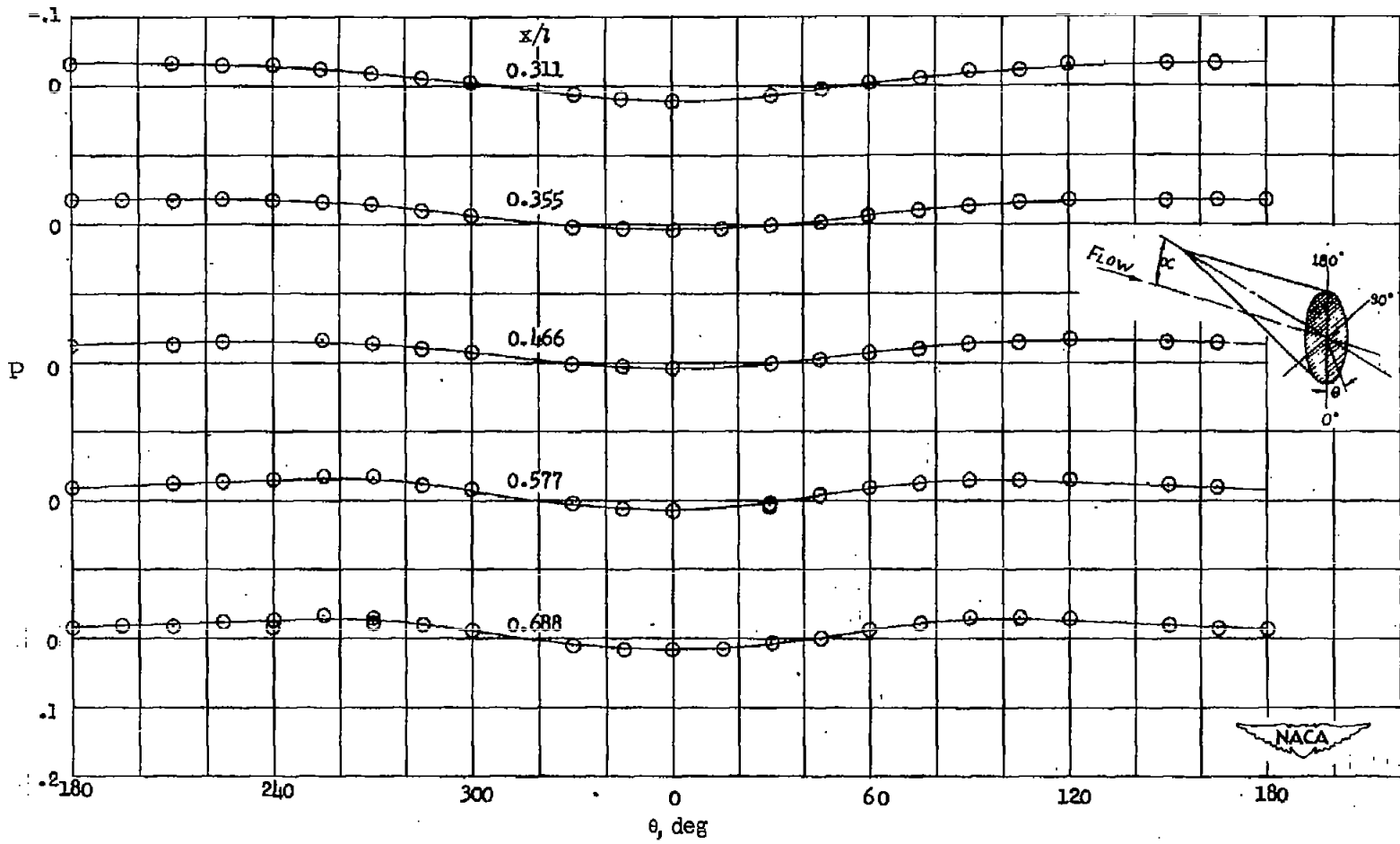
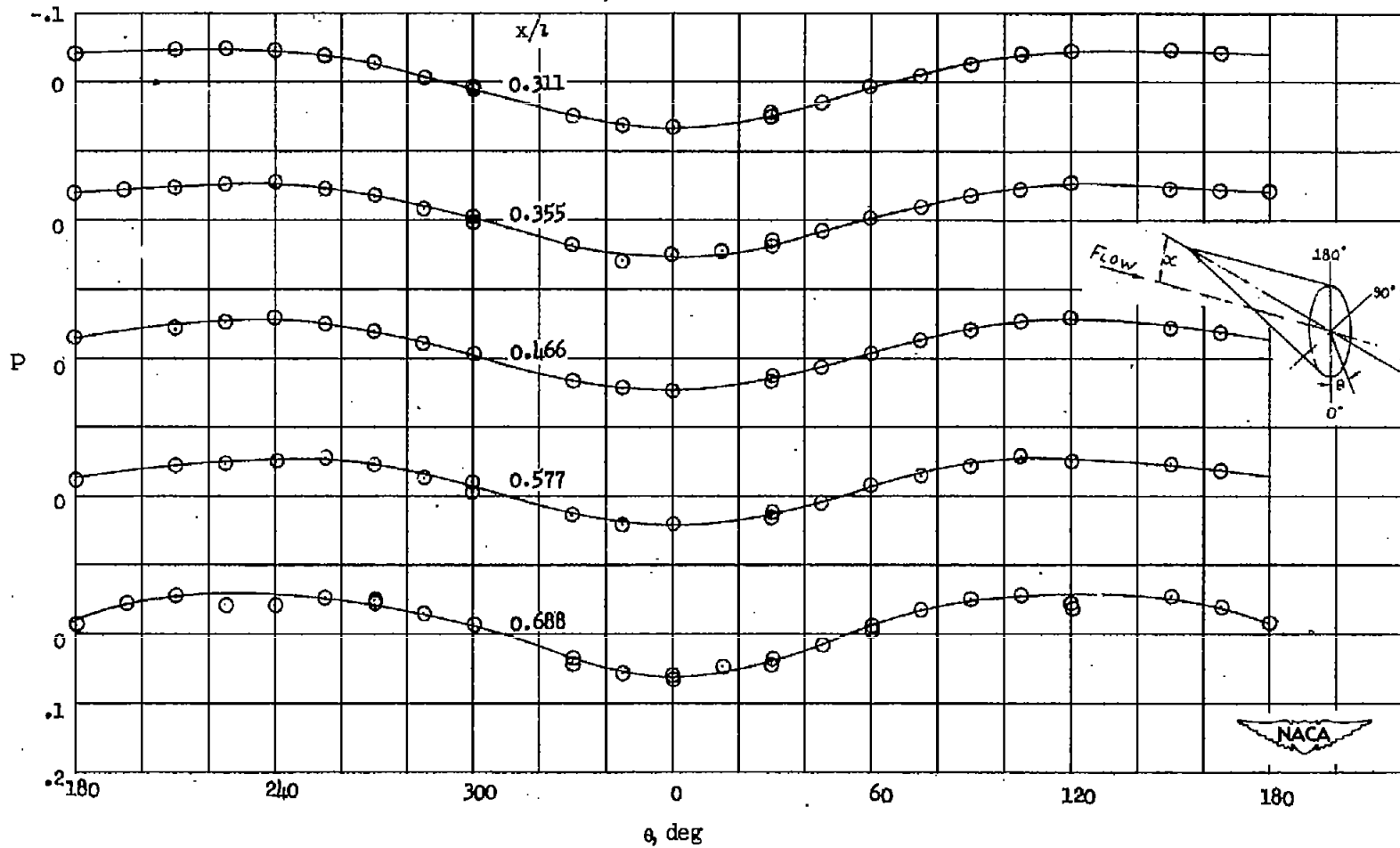
(a)  $\alpha = 0^\circ$ .

Figure 9.- Experimental circumferential pressure distributions for several longitudinal stations.  $M = 4.04$ ;  $R = 19 \times 10^6$ .



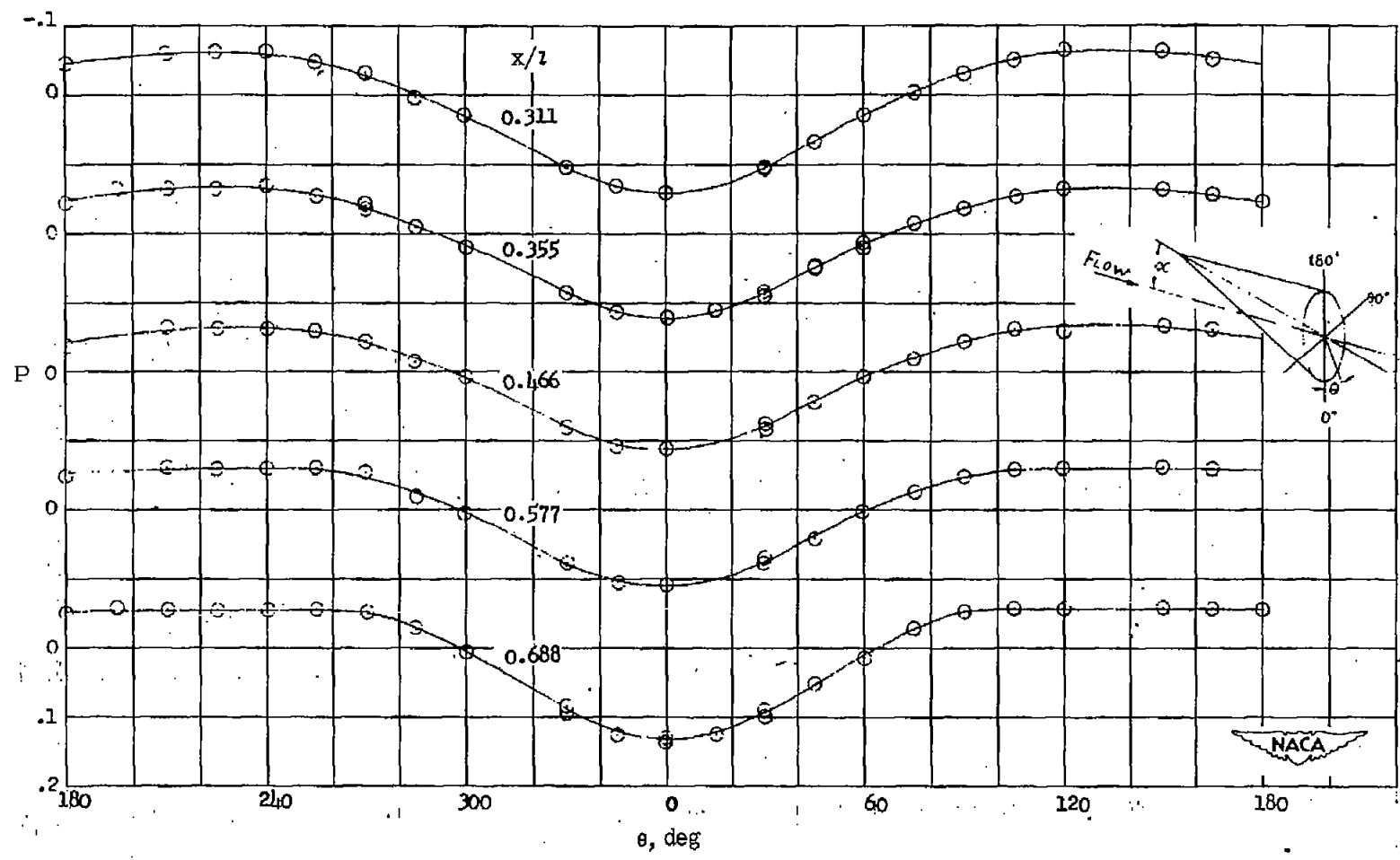
(b)  $\alpha = 5^\circ$ .

Figure 9.- Continued.



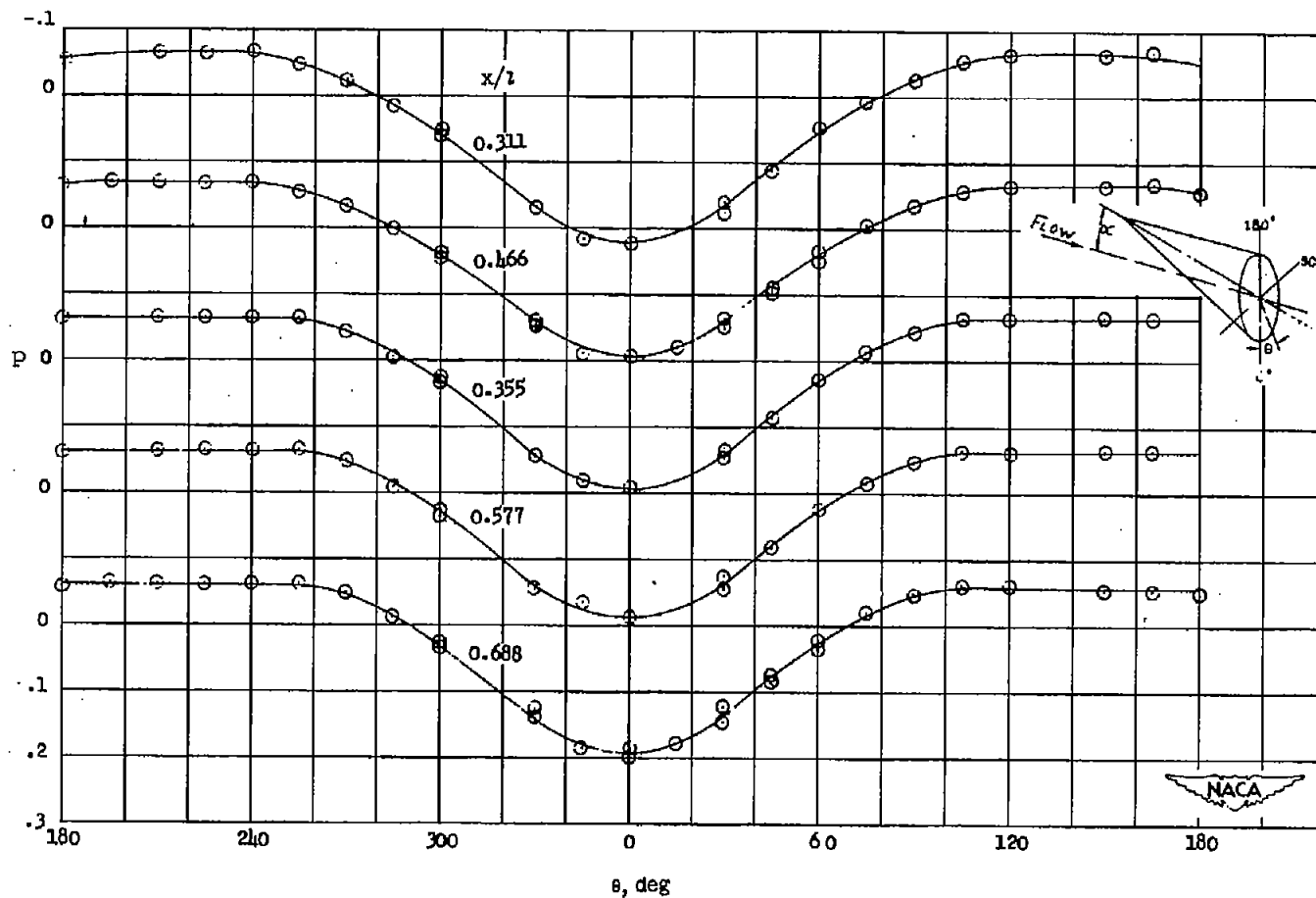
(c)  $\alpha = 10^\circ$ .

Figure 9.- Continued.



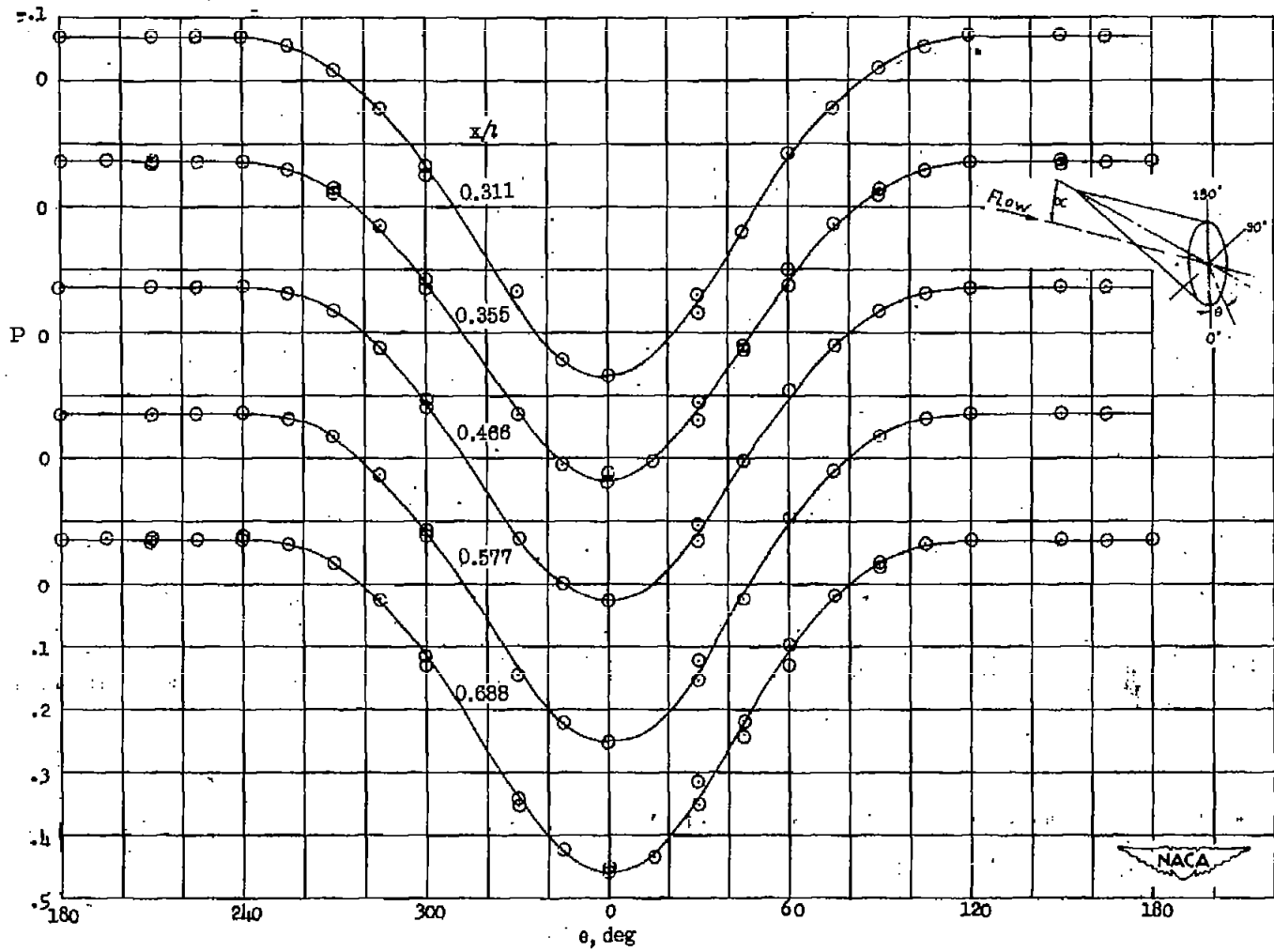
(d)  $\alpha = 15^\circ$ .

Figure 9.- Continued.



(e)  $\alpha = 20^\circ$ .

Figure 9.- Continued.



(f)  $\alpha = 30^\circ$ .

Figure 9. - Concluded.

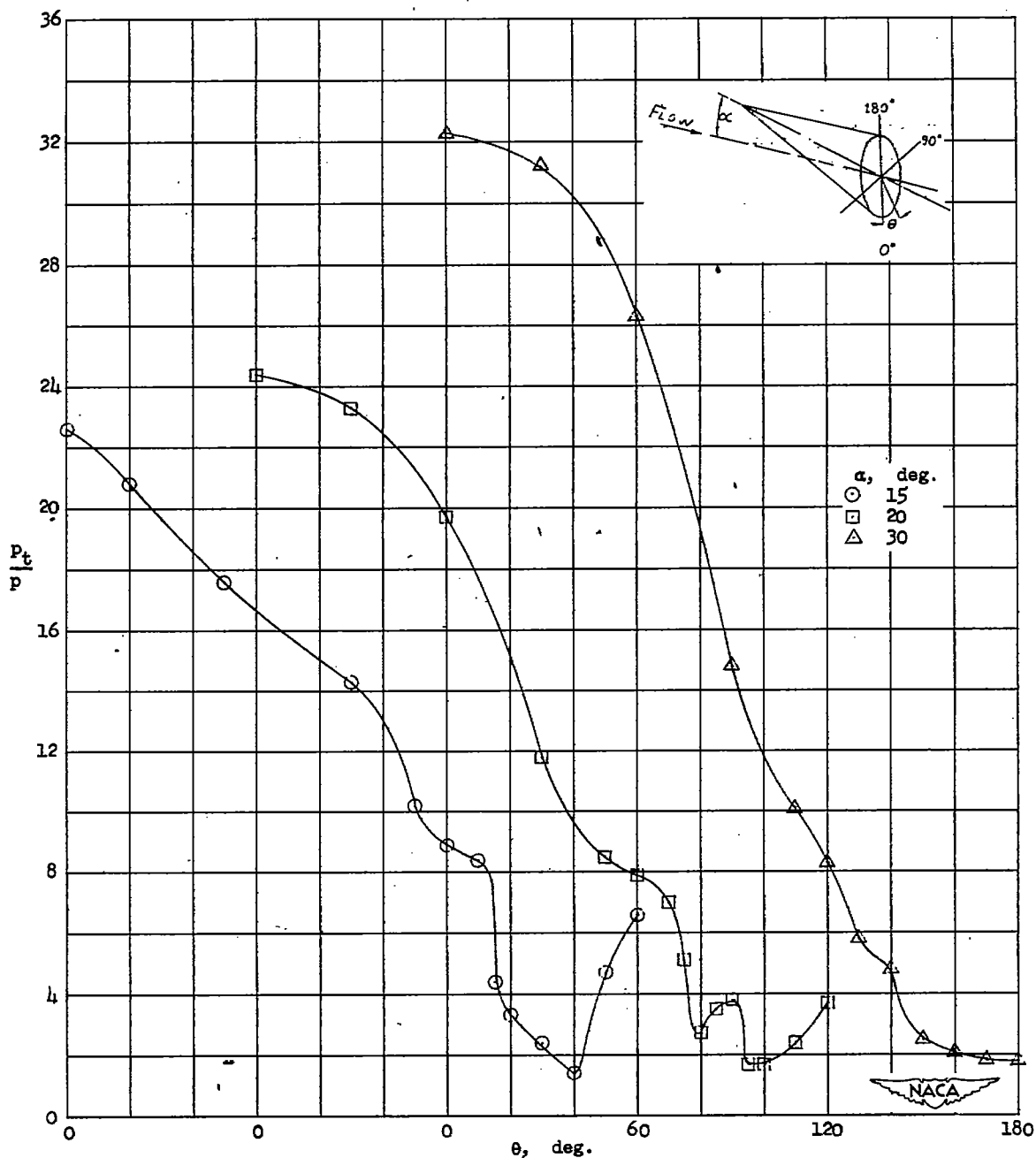
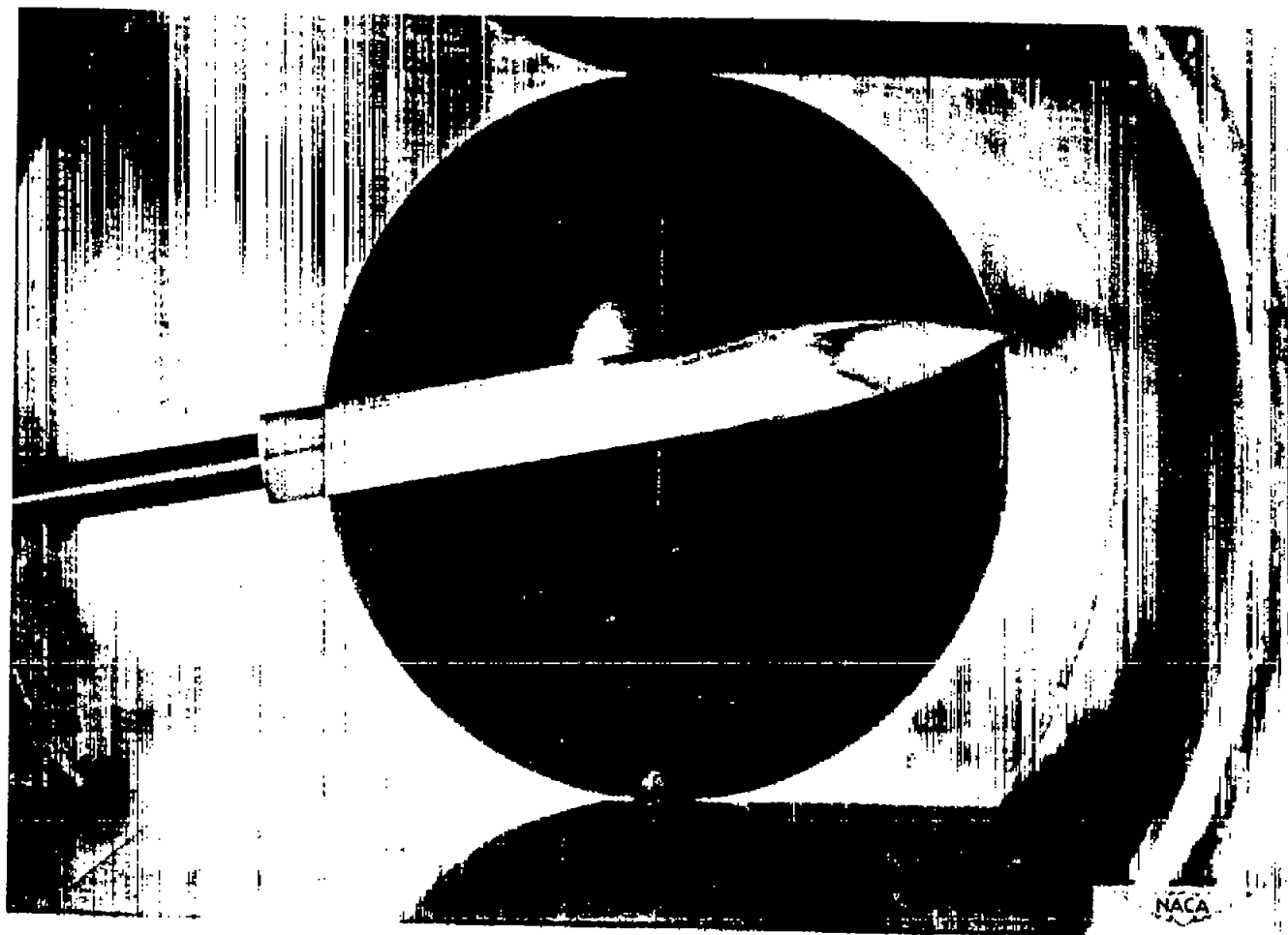
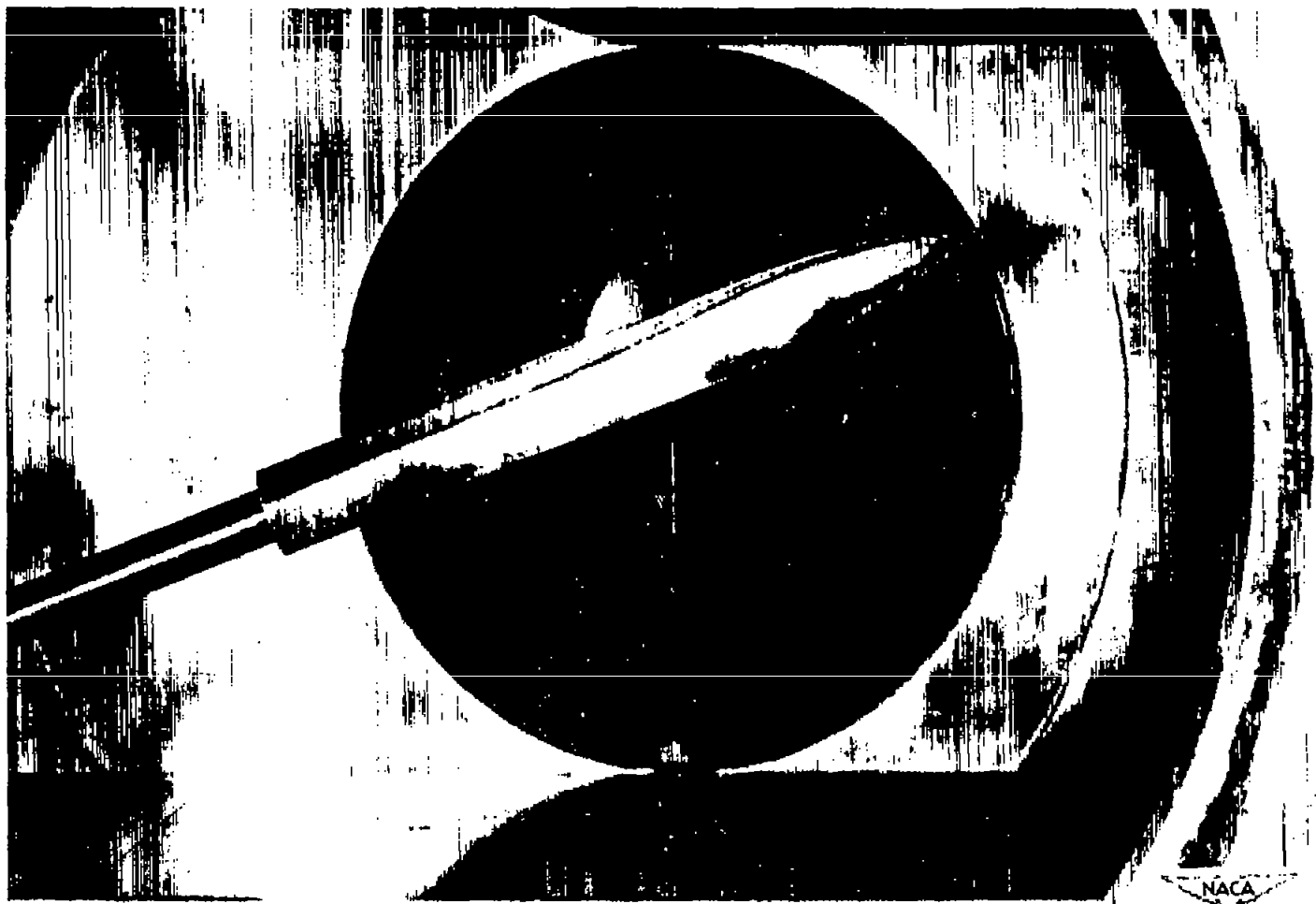


Figure 10.- Surveys of the total pressure around the body at the 72.2-percent-body-length station at 0.19 diameter from the body surface.  $M = 4.04$ ;  $R = 19 \times 10^6$ .



(a)  $\alpha = 10^\circ$ .

Figure 11.- Photographs of model immediately after runs using the china-clay lacquer technique.



(b)  $\alpha = 20^\circ$ .

Figure 11.- Continued.



(c)  $\alpha = 30^\circ$ .

Figure 11.- Concluded.

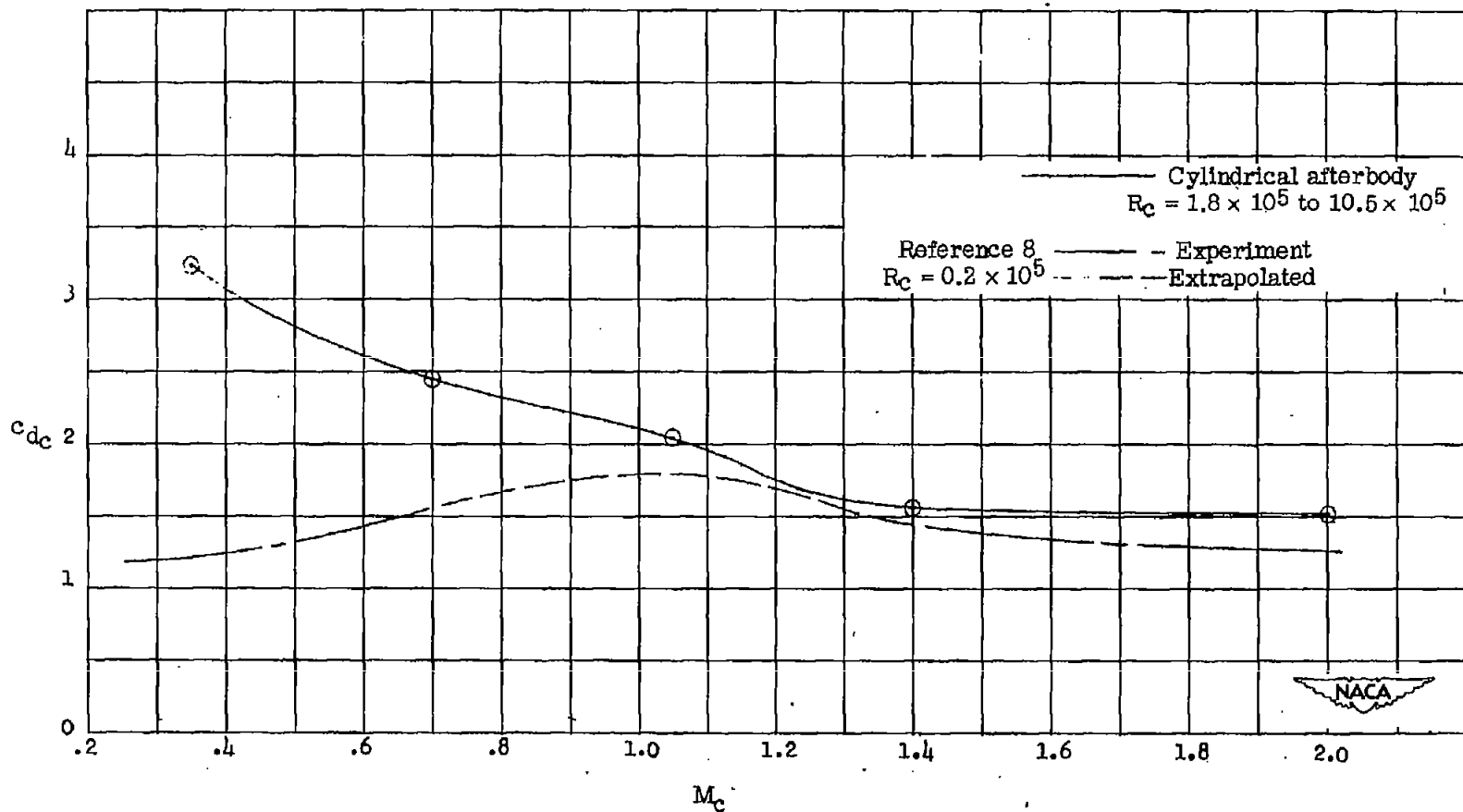


Figure 12.- Variation of the cylindrical section cross-drag coefficient at the 68.8-percent-body-length station with the cross component of the stream Mach number.  $M = 4.04$ ;  $R = 19 \times 10^6$ .